International Journal of Microwave and Wireless Technologies

cambridge.org/mrf

Characterization and Comparison of Formulas for Optimizing Broadside Radiation and Null Beams in 2D Leaky-Wave Antennas

Walter Fuscaldo[1], David R. Jackson[2] and Alessandro Galli[3]

[1]Istituto per la Microelettronica e i Microsistemi, Consiglio Nazionale delle Ricerche, Rome, Italy; [2]Department of Electrical and Computer Engineering, University of Houston, Houston, TX, USA and [3]Department of Information Engineering, Electronics and Telecommunications, Sapienza University of Rome, Rome, Italy

Research Paper

Cite this article: Fuscaldo W, Jackson DR, Galli A (2025) Characterization and Comparison of Formulas for Optimizing Broadside Radiation and Null Beams in 2D Leaky-Wave Antennas. *International Journal of Microwave and Wireless Technologies* **17**(5), 874–880. https://doi.org/10.1017/S1759078724001338

Received: 30 September 2024
Revised: 3 December 2024
Accepted: 5 December 2024

Keywords:
Fabry–Perot cavity antennas; Leaky waves; Leaky-wave antennas; Partially reflecting sheets; Pencil beams; Radiation patterns

Corresponding author: Walter Fuscaldo; Email: walter.fuscaldo@cnr.it

Abstract

Two-dimensional (2D) leaky-wave antennas (LWAs) are commonly designed to radiate pencil beams at broadside and/or scanned conical beams. Recently, the possibility to radiate narrow null patterns at broadside has also been preliminarily explored. In this work, we first review the design rules to obtain a pencil beam from an infinite 2D LWA and then show how they change for having a beam with a narrow null at broadside. The effects of antenna truncation are also accounted for in both cases, and numerical results show how the optimum conditions are in turn affected. Finally, full-wave validations of practical structures excited with either horizontal or vertical dipoles validate the analysis.

Introduction

Two-dimensional (2D) leaky-wave antennas (LWAs) are a wide class of LWAs commonly based on a grounded dielectric slab with a partially reflecting surface (PRS) on top [1]. The PRS may take various forms, e.g., a *homogenized* PRS (i.e., a subwavelength periodic patterning of a thin metal plate), a quarter-wavelength dielectric superstrate, a multilayered stack of alternating high-/low-index quarter-wavelength dielectric layers, etc. [1, 2]. Regardless of its implementation, in all these cases, as far as the layers are assumed to be lossless, it is always possible to model the PRS with a shunt susceptance B_s in the transverse equivalent network. This assumption restricts the analysis to quasi-uniform 2D LWAs. The latter are typically based on a Fabry–Perot cavity structure and are fed at the center with a source, typically modelled as a simple dipole source [2].

The type of dipole source strongly determines the radiation properties of a 2D LWA [3]. As shown in [4], a pencil beam at broadside can only be obtained if both transverse-electric (TE) and transverse-magnetic (TM) leaky modes are excited in the cavity, and the ratio between the amplitudes equals that between their respective leaky wavenumbers. Fortunately, this condition is met by exciting the structure with a horizontal electric (magnetic) dipole in the middle of the cavity (on the ground plane). Conversely, a vertical electric (magnetic) dipole on the ground plane (in the middle of the cavity) can never produce a pencil beam: an omnidirectional pattern with a null at broadside is instead obtained because of the symmetry of the source.

Most of the works on 2D LWAs are focused on techniques for obtaining the highest gain at broadside [5–8], hopefully over the largest bandwidth [9, 10]. The interest in null patterns has been recently revitalized by the work in [11], where a periodic one-dimensional (1D) LWA capable of steering a narrow null has been proposed for direction-of-arrival and antijamming applications. In both contexts, it is important to simultaneously have a sharp null and a high gain to maximize the monopulse difference slope and in turn minimize the angle error [12]. In this respect, 2D LWAs can offer a significant advantage with respect to 1D LWAs because they notably feature a higher gain. However, 2D LWAs capable of radiating a narrow null beam were not explored in the past, although a preliminary theoretical investigation has been proposed at EuCAP 2023 by these authors [13].

As a considerable step forward with respect to the analysis in [13], we show how the antenna truncation affects the beam properties and in turn the optimization conditions in 2D LWAs radiating either a fixed narrow pencil beam or a narrow null beam at broadside. In particular, *optimum* values of the leaky phase and attenuation constants that minimize the half-power beamwidth (HPBW) and the half-power nullwidth (HPNW) are studied for different antenna aperture radii. Similar to finite-size 1D bidirectional LWAs [14–17], the antenna truncation may considerably affect such optimum values. A preliminary investigation on these aspects was provided in an earlier version of this paper that was presented at the 18th European Conference on

© The Author(s), 2024. Published by Cambridge University Press in association with The European Microwave Association. This is an Open Access article, distributed under the terms of the Creative Commons Attribution licence (http://creativecommons.org/licenses/by/4.0), which permits unrestricted re-use, distribution and reproduction, provided the original article is properly cited.

Antennas and Propagation (EuCAP 2024) and was published in its proceedings [18]. A thorough modal analysis is here provided to investigate the dispersive properties of all the leaky modes excited in the structure and their relation to the radiation patterns. A full-wave analysis is also included to analyze the effects of the boundary conditions at the radial edge, as well as to corroborate the accuracy of the proposed leaky-wave approach.

A brief overview of the problem is reported in Section 2, whereas numerical results are reported in Section 3 for both the infinite and finite (truncated) cases. Section 4 reports full-wave validations of practical structures and their comparison against the theoretical expectations. Conclusions are drawn in Section 5.

Theoretical framework

The reference antenna structure is reported in Fig. 1 and consists of a grounded dielectric slab with a PRS on top. When excited with a vertical electric dipole or a horizontal magnetic dipole on the ground plane (VED or HMD), it produces a null or a pencil beam at broadside, respectively. (Similar results apply for a vertical magnetic dipole (VMD) and a horizontal electric dipole (HED) in the middle of the cavity.) As shown in [13], for an infinite structure, the normalized leaky-wave far-field power pattern of 2D LWA fed with an HMD source has the following expression [4] (as a consequence of [4, Eq. (33)] under the condition [4, Eq. (35)]):

$$P_{\mathrm{HMD}}(\theta) = \frac{1}{|\hat{k}_\rho^2 - \sin^2\theta|^2}, \tag{1}$$

where θ is the elevation angle (measured from the vertical z-axis) and $\hat{k}_\rho = \hat{\beta} - j\hat{\alpha}$ is the normalized (with respect to the free-space wavenumber $k_0 = 2\pi/\lambda_0$, λ_0 being the free-space wavelength) *leaky* wavenumber, with $\hat{\beta}$ and $\hat{\alpha}$ being the normalized leaky phase and attenuation constants. When the excitation is a VED source, the normalized leaky-wave far-field power pattern reads [13]:

$$P_{\mathrm{VED}}(\theta) = \sin^2\theta P_{\mathrm{HMD}}(\theta). \tag{2}$$

(The radiated far field from the VED will be polarized in the E_θ direction.) When the antenna is of finite radius R (assumed to be truncated by ideal absorber at this radius), these formulas might not be accurate, especially for low values of the radiation efficiency e_r. For 2D LWAs, an exact formula for the radiation efficiency is not available, but it is typically evaluated with the same formula used for 1D bidirectional LWAs [15], viz., $e_r \simeq 1 - \exp(-2\alpha R)$. Formulas for the radiation patterns in the finite case are provided in [4] and are not repeated here for brevity.

Numerical results

A comprehensive analysis of the optimum conditions should consider the simultaneous variation of the relative permittivity ε_r, the PRS susceptance B_s, the antenna radius R, the cavity height h, and the operating frequency f. In this regard, we should stress that, as far as we assume a nondispersive behavior for B_s (a reasonable assumption for the small fractional bandwidths examined in this work), the optimization with respect to h or f are two sides of the same coin: results will look the same in terms of a *normalized* cavity height h/h_0 or frequency f/f_0 where h_0 and f_0 represent the optimum cavity height and frequency, respectively for obtaining maximum radiated power at broadside in an infinite 2D LWA [19]. This condition also corresponds to the leaky cutoff of a Fabry–Perot cavity (FPC) LWA, i.e., when $r \equiv \hat{\beta}/\hat{\alpha} = 1$.

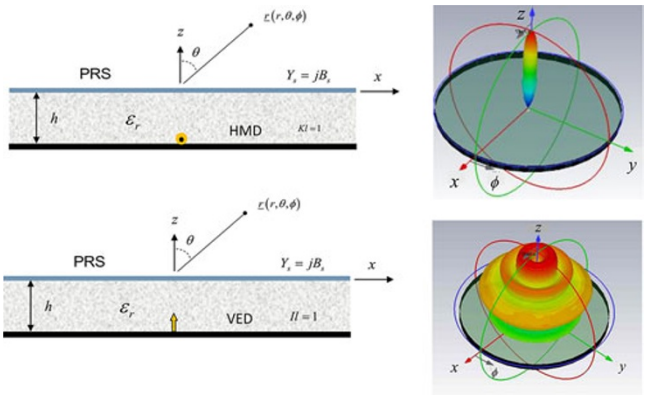


Figure 1. Side views of a typical 2D LWA are reported on the left, fed with an HMD (top left) and a VED (bottom left) on the ground plane. On the right side are corresponding representative patterns. The HMD produces a pencil beam at broadside, while the VED produces a narrow null pattern at broadside.

Equations for obtaining h_0 as a function of the other parameters have already been provided in [20] and can be expressed as:

$$\frac{h_0}{h_{\mathrm{PPW}}} = \mathrm{Re}\left[1 + \frac{1}{\pi}\cot^{-1}\left(\frac{B_s\eta_0 - j}{\sqrt{\varepsilon_r}}\right)\right], \tag{3}$$

with

$$h_{\mathrm{PPW}} = \frac{c}{2f_0\sqrt{\varepsilon_r}} = \frac{\lambda_0|_{f=f_0}}{2\sqrt{\varepsilon_r}}, \tag{4}$$

c being the speed of light in vacuum. (Although derived in [20] for a 1D PRS LWA, the same result holds for a 2D PRS LWA.) Equation (4) corresponds to the cutoff condition of the equivalent parallel-plate waveguide (PPW) structure obtained for $B_s \to \infty$. With these two equations (viz. (3) and (4)) at hand, the antenna designer has multiple choices to optimize the structure. If the cavity thickness h_0 is provided as a requirement, h_{ppw} can be obtained from (3), and used to obtain the optimum frequency from (4). Vice versa, if the frequency f_0 is provided as a requirement, h_{ppw} can be obtained from (4) and used to obtain the optimum cavity thickness from (3).

In the following, we consider the air-filled case $\varepsilon_r = 1$ and fix $\bar{B}_s \equiv B_s\eta_0 = 20$ where $\eta_0 \simeq 377\,\Omega$ is the free-space impedance, and $f_0 = 60$ GHz. For this choice of parameters, we set $h_0/\lambda_0 = 0.5079$ according to (3) and explore the optimum normalized frequency f/f_0 to get either the minimum HPBW or the minimum HPNW. The HPNW is defined as twice the angle between the null angle (broadside) and the angle where the power pattern is down by 3 dB from that at the peak of the conical beam. The minimum HPBW condition is known to occur in *infinite* 2D LWAs for $r \simeq 0.5176$ [13, 19]. Conditions for minimum HPBW in *finite-size* 2D LWAs and for minimum HPNW in both infinite and finite-size 2D LWAs are, instead, new. From the analysis of this case, similar conclusions can be drawn for other choices of B_s, ε_r, and f_0.

Examining the complex wavenumbers helps provide insight into the radiation performance. Taking advantage of the azimuthal symmetry of the considered 2D LWAs, we obtained the dispersion equations in the TE and the TM cases by considering a 1D transverse section of the structure. The expressions are obtained in compact form in [20] and reported here for the reader's convenience (assuming an air substrate):

$$\mathrm{TE}: (j\bar{B}_s + \hat{k}_z)\frac{\sin(k_0 h\hat{k}_z)}{\hat{k}_z} - j\cos(k_0 h\hat{k}_z) = 0 \tag{5}$$

https://doi.org/10.1017/S1759078724001338 Published online by Cambridge University Press

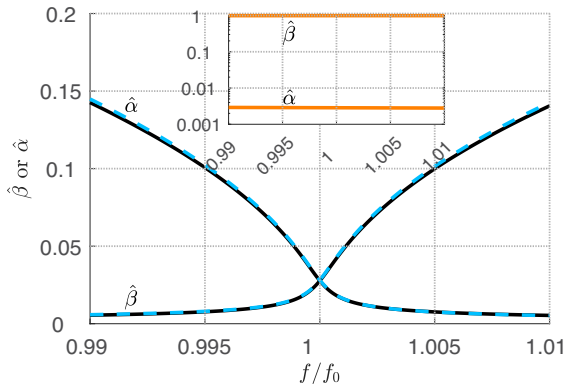


Figure 2. Dispersion curves $\hat{\beta}$ and $\hat{\alpha}$ vs. f/f_0 of the fundamental TM-TE leaky mode pair (TM in solid black line, TE in dashed light blue line) and the quasi-TEM leaky mode (in solid orange line in the inset).

$$\text{TM}: (j\bar{B}_s + \hat{k}_z^{-1}) \sin(k_0 h \hat{k}_z) - \frac{j\cos(k_0 h \hat{k}_z)}{\hat{k}_z} = 0, \qquad (6)$$

where $\hat{k}_z = \sqrt{1 - \hat{k}_\rho^2}$ is the vertical wavenumber in free space. (The radical sign (principal square root) ensures the improper choice of wavenumber in the air.) We numerically solved the dispersion equations above for both TE and TM leaky modes for various values of f in the range $0.99 \leq f/f_0 \leq 1.01$, which correspond to values of r in the range $0.04 \leq r \leq 25$. The dispersion curves for the fundamental TE-TM leaky mode pair (dashed light blue and solid black line, respectively) are shown in Fig. 2. In the case of a VED excitation, only the fundamental TM and an extra quasi transverse electromagnetic (TEM) leaky mode are excited, whereas for an HMD excitation, all modes are excited. In addition, for the optimum frequency f_0, we decided to inspect the behavior of the TE and TM dispersion equations as functions of $\hat{\beta}$ and α in the range $0 < \hat{\beta} < 1.5$, $|\hat{\alpha}| < 0.05$ to verify the presence of other zeros (or, equivalently, poles of the relevant dyadic Green's functions of the structure) over the proper ($\text{Im}\{\hat{k}_z\} < 0$) and improper ($\text{Im}\{\hat{k}_z\} > 0$) Riemann sheets (see Fig. 3(a)–(d)). We recall here that leaky modes possess a *quadrantal symmetry* for a lossless planar stratified structure [21, 22]: given a leaky mode with complex wavenumber $k_{\text{LW}} = \beta_{\text{LW}} - j\alpha_{\text{LW}}$, the solutions $\pm k_{\text{LW}}$ and $\pm k_{\text{LW}}^*$ are also mathematically found. In our problem, we only consider solutions with $\beta_{\text{LW}} > 0$ and refer to the solution with $\alpha_{\text{LW}} > 0$ ($\alpha_{\text{LW}} < 0$) as a *physical* (*nonphysical*) leaky mode [23]. (Here, with *nonphysical* we refer to leaky-wave solutions that exponentially grow along the radial direction.) In the representation of Fig. 3(a)–(d), for each leaky mode, we thus see a *complex conjugate* leaky-mode pair (the remaining two mathematical solutions are not displayed because we only consider solutions with $\beta > 0$).

This analysis proved to be very useful to find another TM leaky mode which appears quite close to the branch point, i.e., $\hat{k}_\rho = 1$ (see the two narrow dark dips in Fig. 3(a)). This is the quasi-TEM leaky mode that exists in an air-filled Fabry–Perot cavity and which may contribute to endfire radiation, as will be shown next in Section 4. The frequency dispersion of this quasi-TEM leaky mode is then obtained by solving again the TM dispersion equation, providing the wavenumber of the unperturbed TEM parallel-plate waveguide mode as initial guess, and is reproduced with solid orange lines in the inset of Fig. 2.

The fundamental TE-TM leaky-mode pair and the quasi-TEM leaky mode are the only three modes supported by this structure, as can be inferred from Fig. 3(a)–(d). In this regard, we should note that the weak dip appearing in the proper sheet for the TM case is not due to a pole, but is simply part of the natural variation of the function. In the TM case the function actually tends to infinity at the branch point, but this is not seen due to the sample density in the plot.

Since we are interested in 2D LWAs radiating at broadside we will now examine the contribution of the fundamental TE-TM leaky mode pair only. Specifically, for each value of f, we evaluated the radiation patterns (a few relevant examples are shown in Fig. 4(a)–(b)) considering either a VED or an HMD source for the infinite case (through (1) and (2), respectively), $R \to \infty$ and for $R = 5\lambda_0$, $10\lambda_0$, $15\lambda_0$, $20\,\lambda_0$ (through [4, Eqs. (10)–(12)] and [4, Eqs. (24)–(34)] for the VED and HMD cases, respectively). For each broadside pattern (HMD case) we evaluated the HPBW, whereas for each null pattern (VED case), we evaluated the HPNW. Both the HPBW and HPNW are then normalized to the HPBW obtained from a 2D LWA when $r = 1$, which is equal to $2\sqrt{2}\hat{\alpha}$. These normalized beamwidths $\overline{\text{HPBW}}$ and $\overline{\text{HPNW}}$ are then reported in Fig. 4(c)–(d) as functions of r for the different choices of R. The different values of r were obtained by changing the substrate thickness while keeping the frequency fixed at 60 GHz. Colored circles denote the values of r that give the minimum beamwidths or nullwidths. (Circles are not shown for the two smallest apertures (the black and red curves), since either the minima are off the plotted scale, or the curves are so flat for the larger r values that the minimum is inconsequential.)

In this regard, it is worthwhile to stress that the radiation patterns of infinite 2D LWAs are similar to those of 1D infinite bidirectional LWAs, and thus the beamsplitting and dual-beam conditions are expected to occur for $r > 1$ and $r > 1+\sqrt{2} \simeq 2.414$, respectively. As a result, for values of $r > 2.414$, it is not always possible to have a well-defined HPBW at broadside. However, as we consider finite-size 2D LWAs, these boundaries are expected to change, although for 2D LWAs a rigorous examination as those provided in [14, 15] is still lacking and will be subject of future studies. Therefore, results for $r \gg 1$ have to be taken with care, and this is the reason why we reported results in the limited range $0 < r < 2.5$.

The results for the normalized HPBW in the infinite case agree with the theoretical expectations: the minimum is found approximately at $r = 0.5176$ and at $r = 1$ the normalized HPBW approaches unity, as per definition (see Fig. 4(c)). In this regard, we should recall that 0.5176 is actually an approximation of the exact minimum HPBW condition for the infinite-aperture case, which reads $r = \sqrt{2 - \sqrt{3}}$ as shown in [19]. Remarkably, this quantity, viz., $\sqrt{2 - \sqrt{3}}$, is also connected to another condition, as it represents the ratio between the HPNW and the HPBW when $r = 1$, i.e., $\overline{\text{HPNW}}(r = 1) \simeq 0.5176$ (see the gray curve in Fig. 4(d)) as already discussed in [13]. The behavior of the HPNW/HPBW ratio as a function of r can be inferred from Fig. 4(c) and (d): the HPNW/HPBW ratio in the infinite case increases for $r \to 0$ reaching values as large as 0.64.

The results in the finite case are rather interesting. As R decreases, the minimum region becomes less pronounced (the curve becomes flatter) and the minimum condition shifts to higher values of r. Even for a rather electrically large antenna of radius equal to $15\lambda_0$, the minimum HPBW occurs at values of r close to 1

https://doi.org/10.1017/S1759078724001338 Published online by Cambridge University Press

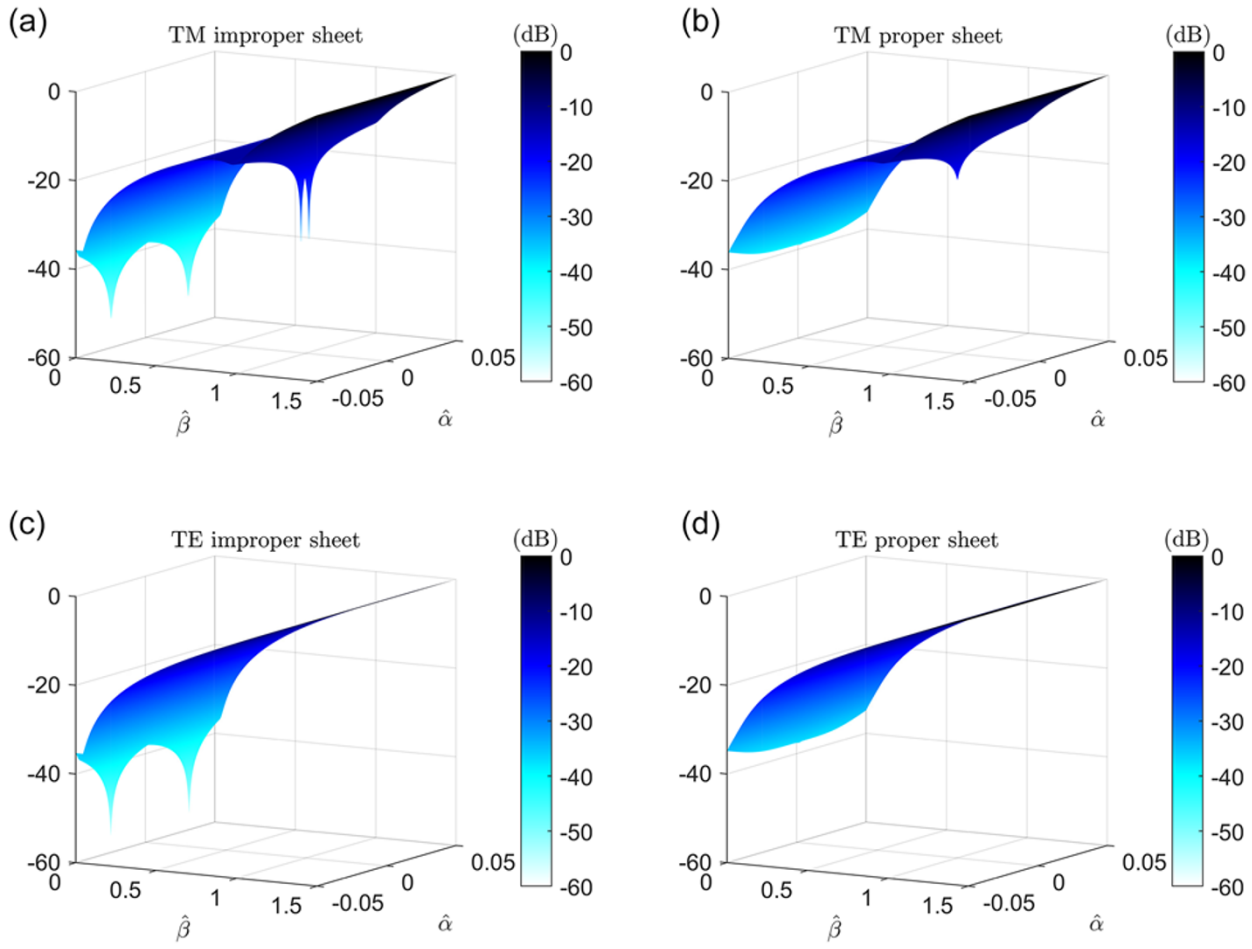


Figure 3. Normalized surface plots of the magnitude of the dispersion equation (the left-hand side of (5) or (6)) as a function of $\hat{\beta}$ and $\hat{\alpha}$ reported in dB scale (i.e., $10\log(\cdot)$) for the following cases: (a) TM, improper sheet, (b) TM, proper sheet, (c) TE, improper sheet, (d) TE, proper sheet. Pole singularities of the relevant 1D Green's functions correspond to zeroes of the dispersion equation and look as sharp minima in this representation. Leaky-mode solutions appear as a complex conjugate pair in the TM and TE cases for the improper sheet. The weak dip appearing in the TM case for the proper sheet is due to the presence of the branch-point singularity at k_0.

rather than 0.5176. It is seen that for small apertures, e.g., $R = 5\lambda_0$, the normalized HPBW is only slightly affected by increasing r beyond 1. The beam narrowing for the sought conditions can also be appreciated from Fig. 4(a) where the leaky radiation patterns for the infinite case (in gray) and the finite case with $R = 20\lambda_0$ (in blue) are shown for $r = 1$ and the value of r that leads to minimum beamwidth for the infinite and finite cases.

Similar considerations can be drawn for the normalized HPNW (see Fig. 4(b) and (d)). Again, as R decreases, the minimum region becomes less pronounced and the minimum condition shifts to higher values of r (see Fig. 4(d)). However, the HPNW is much less affected by variations of r, the region of the curves near the minimum being very flat. Interestingly, for the infinite case, the condition for the minimum HPNW differs from that for the minimum HPBW and it is found to be about $r = 0.6258$ (see the gray curve in Fig. 4(d)). In conclusion, the range $0.5 \leq r \leq 1$ seems appropriate if the goal is the minimization of either the HPBW or the HPNW, whatever the aperture size is. The weaker sensitivity of the nullwidth with respect to the beamwidth to variations of r and of the lateral truncation are also manifest in 4(b) where it is seen that the condition for minimum nullwidth only slightly narrows the null region with respect to the condition that leads to maximum radiated power at broadside, viz., $r = 1$. As for the HPNW/HPBW ratio, it is noted that as R decreases the HPNW/HPBW ratio (for $r = 1$) shows a rather constant behavior, and the value slightly increases with respect to the value of 0.5176 found in the infinite case. To give some numbers: for $R = 5\lambda_0$, we have HPNW/HPBW = 0.73, for $R = 10\lambda_0$ we have HPNW/HPBW = 0.68.

Full-wave validation

Results from previous sections discussed results from either an infinite structure or one terminated with ideal absorber. This section aims at bringing the previous analysis to a more practical level. First, we demonstrate with full-wave simulations that the leaky-wave pattern provides a remarkably accurate representation of the total pattern near the peak. Second, we investigate the effect of the lateral truncation when different boundary conditions are considered.

For this purpose, we designed in CST the 2D LWA described in the previous section with $R = 6.6\lambda_0$ which approximately leads to a radiation efficiency of 90% at f_0; a typical criterion for the design of practical 2D LWA [1, 3]. The PRS is implemented as a surface impedance boundary condition (SIBC) with $B_s = 20\eta_0$ at f_0. This assumption is well satisfied by typical PRS in the homogenized regime, such as patch arrays [24]. Therefore, the use of the SIBC in place of the patterned PRS allows for saving significant computational resources without affecting the accuracy of the results, as already shown in [20] where this approach has been used to simulate a 1D LWA based on a metal strip-grating PRS.

https://doi.org/10.1017/S1759078724001338 Published online by Cambridge University Press

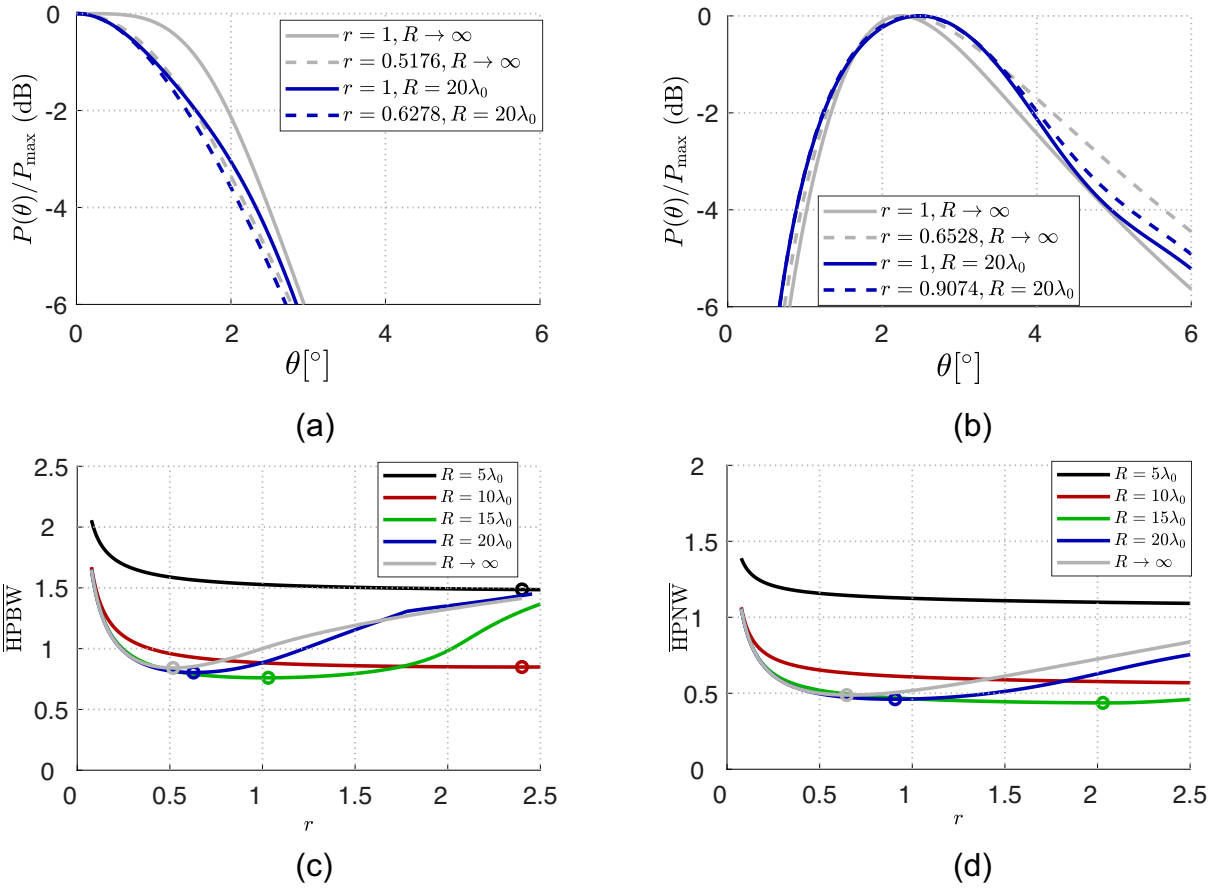


Figure 4. (a)–(b) Normalized *leaky* radiation patterns for $r = 1$ (solid lines) and $r = 0.5176$ (dashed lines) for the infinite case, i.e., $R \to \infty$ (in gray) and for $R = 20\lambda_0$ (in blue). (a) HMD case and (b) VED case. (c)–(d) Normalized half-power beamwidth and normalized half-power nullwidth vs. r for different values of the aperture radius R. A colored circle highlights the minimum beamwidth or nullwidth for each curve.

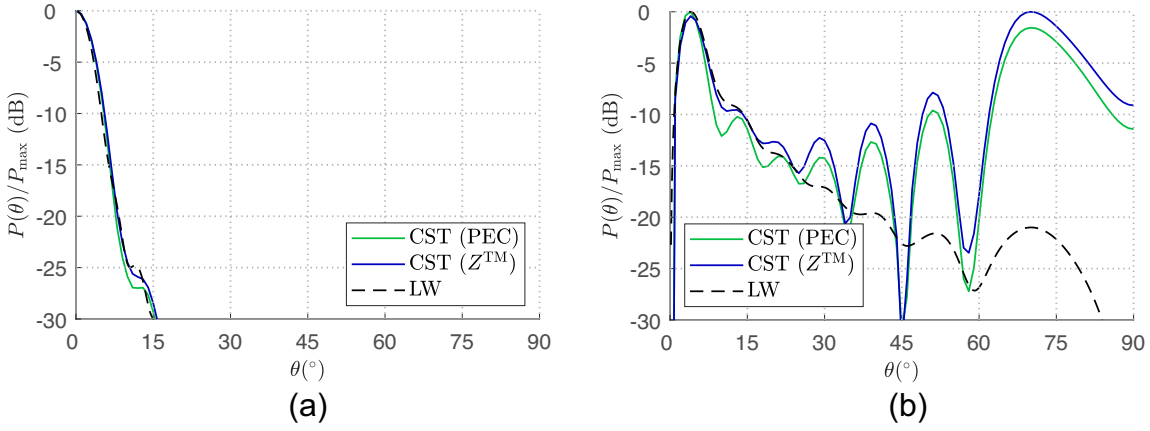


Figure 5. (a)–(b) Normalized leaky radiation patterns (in dashed black line) for (a) the HMD case and (b) the VED case, compared against normalized *total* (CST) radiation patterns when a PEC boundary condition (in solid green line) and an SIBC (in solid blue line) matching the wave impedance of the TM leaky mode are applied to the radial edge.

At the lateral edge, two different boundary conditions are considered: (i) a perfect electric conductor (hereafter referred as "PEC"), and (ii) an SIBC (hereafter referred as "Z_{TM}") using the wave impedance of the radially propagating TM leaky mode in the leaky radial waveguide (see [25, Eq. (5.38)] for $n = 1$). (These boundary conditions extend from the ground plane to the PRS at the lateral edge.) We should stress that the latter condition acts as a nearly perfect absorbing surface for VED excitation, but not for HMD excitation. In this latter case, both TE and TM leaky modes are excited and the wave impedance of a TE mode is different than of a TM mode [25, cf., Eqs. (5.38)–(5.40)]).

The structure fed with either a simple VED or a simple HMD is finally simulated considering the two different lateral boundary conditions, and the resulting *total* far-field patterns at f_0 are compared against the theoretical *leaky* patterns in Fig. 5(a)–(b). (The leaky-wave patterns are based on the dominant leaky waves,

https://doi.org/10.1017/S1759078724001338 Published online by Cambridge University Press

and ignore the quasi-TEM leaky wave that is a TM wave.) More precisely, a 1D cut at $\phi = 0^\circ$ of the power pattern normalized to its maximum is reported in Fig. 5(a)–(b). (Results look very similar for $\phi = 90^\circ$ in the case of HMD excitation, and for any ϕ in the case of VED excitation thanks to the azimuthal symmetry of the aperture field.) In the case of HMD excitation (Fig. 5(a)), there are no appreciable differences among the two different lateral boundary conditions, and the leaky-wave pattern agrees very well with the CST pattern. In the VED case, when either the PEC or the Z_{TM} boundary condition is applied, the agreement between the leaky pattern and the CST pattern is satisfactory only near the peak; a secondary peak near endfire is always present. As we discussed in Section 3, this secondary beam is most likely due to the excitation of the quasi-TEM leaky mode that we clearly identified in Fig. 3(a).

This secondary unwanted beam severely hinders the use of 2D LWAs for producing null beams in practical scenarios. Fortunately, there exist several methods for mitigating this issue, each one with its pros and cons. One possibility is to introduce a dielectric filling which converts the quasi-TEM leaky mode into a TM surface wave that no longer radiates, but still substracts power thus reducing the radiation efficiency. In this regard, the use of a waveguide-fed double iris slot originally proposed in [26] or that of reduced surface-wave microstrip circular patches in [27] allow the feed to avoid exciting the TM surface wave. However, both feeders are alternatives to horizontal dipoles, not vertical dipoles, and thus they are not effective for obtaining a null beam at broadside with no endfire radiation. Taking cues from [27], one may consider to feed the cavity with a circular array of vertical dipoles (which still excites a purely TM leaky mode [28]) and place the array at a critical radius $\rho_{\mathrm{c,TM}}$ to avoid exciting the TM surface wave, given by $\rho_{\mathrm{c,TM}} = j_{01}/\beta_{\mathrm{TM}_0}$, where $j_{01} = 2.4048$ is the first root of the $J_0(\cdot)$ Bessel function and β_{TM_0} is the phase constant of the TM_0 surface-wave mode. Another possibility is to excite the structure with a VMD: in this case, there will be no quasi-TEM mode excited (there is no TEM mode coming from TE modes in a PPW) and no TE surface wave is thus excited, and only the fundamental TE leaky mode seen in Fig. 3(c) is excited. However, the practical realization of either a circular array of VEDs or a VMD is not as simple as that of a single VED, the latter being well represented by a coaxial feeder. (A VMD will also radiate an E_ϕ polarized far field instead of an E_θ polarized far field). Possible implementations of VMD sources have recently been proposed and consist of loop antennas [29, 30] and a circular array of radial slots [31] (possibly fed with microstrip lines as in [32]) for designs at microwave frequencies, or a circular waveguide operating in its higher-order TE_{01} mode [33] (a Marié transducer is used to correctly excite this mode while preventing the excitation of other unwanted modes) for operation at (sub-)millimeter-wave frequencies. Although these feeders have all been used for generating TE-polarized Bessel beams, they can suitably be used in Fabry–Perot structures as Bessel-beam launchers and 2D LWAs share a very similar architecture, viz., a grounded dielectric slab with a PRS on top.

Conclusion

The HPBW and HPNW of infinite and finite-size 2D LWAs excited with an HMD or a VED are studied for different choices of the substrate thickness and aperture radius. It is shown that truncation effects substantially affect the optimum conditions that were obtained for the infinite case, as well as the patterns. For either type of source, an optimum truncation can be beneficial for narrowing the beam. However, with a single dipole source only a *fixed* null beam can be produced. Multiple dipole sources, such as a linear array of HMDs, can be considered for *steering* the null, thus making this structure even more attractive for various applications. This possibility will be the object of future studies.

Acknowledgements. This research was partially supported by the European Union under the Italian National Recovery and Resilience Plan (NRRP) of NextGenerationEU, partnership on "Telecommunications of the Future" (PE00000001 – program "RESTART").

Competing interests. The authors declare none.

References

1. **Jackson DR, Caloz C and Itoh T** (2012) Leaky-wave antennas. *Proceedings of the IEEE* **100**, 2194–2206.
2. **Burghignoli P, Fuscaldo W and Galli A** (2021) Fabry–Perot cavity antennas: The leaky-wave perspective [electromagnetic perspectives]. *IEEE Antennas Propag Magazine* **63**, 116–145.
3. **Jackson DR, Burghignoli P, Lovat G, Capolino F, Chen J, Wilton DR and Oliner AA** (2011) The fundamental physics of directive beaming at microwave and optical frequencies and the role of leaky waves. *Proceedings of the IEEE* **99**, 1780–1805.
4. **Ip A and Jackson DR** (1990) Radiation from cylindrical leaky waves. *IEEE Transactions on Antennas and Propagation* **38**, 482–488.
5. **Scattone F, Ettorre M, Sauleau R, Nguyen NT and Fonseca NJG** (2015) Optimization procedure for planar leaky-wave antennas with flat-topped radiation patterns. *IEEE Transactions on Antennas and Propagation* **63**, 5854–5859.
6. **Blanco D, Rajo-Iglesias E, Maci S and Llombart N** (2015) Directivity enhancement and spurious radiation suppression in leaky-wave antennas using inductive grid metasurfaces. *IEEE Transactions on Antennas and Propagation* **63**, 891–900.
7. **Gardelli R, Albani M and Capolino F** (2006) Array thinning by using antennas in a Fabry–Perot cavity for gain enhancement. *IEEE Transactions on Antennas and Propagation* **54**, 1979–1990.
8. **Foroozesh A and Shafai L** (2009) Investigation into the effects of the patch-type FSS superstrate on the high-gain cavity resonance antenna design. *IEEE Transactions on Antennas and Propagation* **58**, 258–270.
9. **Almutawa AT, Hosseini A, Jackson DR and Capolino F** (2019) Leaky-wave analysis of wideband planar Fabry-Pérot cavity antennas formed by a thick PRS. *IEEE Transactions on Antennas and Propagation* **67**, 5163–5175.
10. **Mateo-Segura C, Feresidis AP and Goussetis G** (2013) Bandwidth enhancement of 2-D leaky-wave antennas with double-layer periodic surfaces. *IEEE Transactions on Antennas and Propagation* **62**, 586–593.
11. **Huang M and Liu J** (2022) A null frequency scanning leaky-wave antenna. *IEEE Transactions on Antennas and Propagation* **70**, 7625–7635.
12. **Mailloux RJ** (2005) *Phased Array Antenna Handbook*, Norwood, MA, USA: Artech House.
13. **Fuscaldo W, Galli A and Jackson DR** (2023) Creating sharp nulls at broadside using a 2-D leaky-wave antenna with a vertical dipole source, *European Conference on Antennas and Propagation (EuCAP 2023)*. IEEE: Florence, Italy, pp. 1–2.
14. **Sutinjo A, Okoniewski M and Johnston RH** (2008) Beam-splitting condition in a broadside symmetric leaky-wave antenna of finite length. *IEEE Antennas and Wireless Propagation Letters* **7** 609–612.
15. **Fuscaldo W, Jackson DR and Galli A** (2019) General formulas for the beam properties of 1-D bidirectional leaky-wave antennas. *IEEE Transactions on Antennas and Propagation* **67**, 3597–3608.
16. **Hsu Y-W, Lin H-C and Lin Y-C** (2015) Modeling and PCB implementation of standing leaky-wave antennas incorporating edge reflection for broadside radiation enhancement. *IEEE Transactions on Antennas and Propagation* **64**, 461–468.
17. **Li H-D and Zhu L** (2021) Study on bandwidth properties of EH_1-mode microstrip leaky-wave antenna for broadside radiation. *IEEE Antennas and Wireless Propagation Letters* **20**, 2028–2032.

https://doi.org/10.1017/S1759078724001338 Published online by Cambridge University Press

18. **Fuscaldo W, Jackson DR and Galli A** (2024) Characterization and comparison of formulas for optimizing broadside radiation in a 2-D leaky-wave antenna, *European Conference on Antennas and Propagation (EuCAP 2024)*. IEEE: Glasgow, UK, pp. 1–3.
19. **Lovat G, Burghignoli P and Jackson DR** (2006) Fundamental properties and optimization of broadside radiation from uniform leaky-wave antennas. *IEEE Transactions on Antennas and Propagation* **54**, 1442–1452.
20. **Fuscaldo W, Galli A and Jackson DR** (2022) Optimization of 1-D unidirectional leaky-wave antennas based on partially reflecting sheets. *IEEE Transactions on Antennas and Propagation* **70**, 7853–7868.
21. **Tamir T and Oliner AA** (1963) Guided complex waves. Part 1: Fields at an interface. *Proceedings of the IEEE* **110**, 310–324.
22. **Tamir T and Oliner AA** (1963) Guided complex waves. Part 2: Relation to radiation patterns. *Proceedings of the IEEE* **110**, 325–334.
23. **Fuscaldo W, Burghignoli P and Galli A** (2022) Genealogy of leaky, surface, and plasmonic modes in partially open waveguides. *Physical Review Applied* **17**, 034038.
24. **Luukkonen O, Simovski C, Granet G, Goussetis G, Lioubtchenko D, Raisanen AV and Tretyakov SA** (2008) Simple and accurate analytical model of planar grids and high-impedance surfaces comprising metal strips or patches. *IEEE Transactions on Antennas and Propagation* **56**, 1624–1632.
25. **Harrington RF** (2015) *Time-Harmonic Electromagnetic Fields*, New York, NY, USA: IEEE Press.
26. **Hickey MA, Qiu M and Eleftheriades GV** (2001) A reduced surface-wave twin arc-slot antenna for millimeter-wave applications. *IEEE Microwave and Wireless Components Letters* **11**, 459–461.
27. **Jackson DR, Williams JT, Bhattacharyya AK, Smith RL, Buchheit SJ and Long SA** (1993) Microstrip patch designs that do not excite surface waves. *IEEE Transactions on Antennas and Propagation* **41**, 1026–1037.
28. **Burghignoli P, Fuscaldo W, Comite D, Baccarelli P and Galli A** (2019) Higher-order cylindrical leaky waves—Part I: Canonical sources and radiation formulas. *IEEE Transactions on Antennas and Propagation* **67**, 6735–6747.
29. **Lu P, Voyer D, Bréard A, Huillery J, Allard B, Lin-Shi X and Yang X-S** (2017) Design of TE-polarized Bessel antenna in microwave range using leaky-wave modes. *IEEE Transactions on Antennas and Propagation* **66**, 32–41.
30. **Lu P, Bréard A, Huillery J, Yang X-S and Voyer D** (2018) Feeding coils design for TE-polarized bessel antenna to generate rotationally symmetric magnetic field distribution. *IEEE Antennas and Wireless Propagation Letters* **17**, 2424–2428.
31. **Negri E, Benassi F, Fuscaldo W, Masotti D, Burghignoli P, Costanzo A and Galli A** (2024) Design of TE-polarized resonant Bessel-beam launchers for wireless power transfer links in the radiative near-field region. *International Journal of Microwave and Wireless Technologies* 1–10.
32. **Benassi F, Negri E, Fuscaldo W, Paolini G, Maita F, Burghignoli P, Masotti D, Galli A and Costanzo A** (2024) TE-polarized Bessel-beam launchers for wireless power transfer at millimeter waves: Theory, design, and experimental validation, *IEEE Transactions on Microwave Theory and Techniques*.
33. **Negri E, Fuscaldo W, González-Ovejero D, Burghignoli P and Galli A** (2024) TE-polarized leaky-wave beam launchers: Generation of Bessel and Bessel–Gauss beams. *Applied Physics Letters* **125**(18), 181703.



Walter Fuscaldo received the M.Sc. (cum laude) degree in Telecommunications Engineering from Sapienza University of Rome, Rome, in 2013. In 2017, he received the Ph.D. degree (cum laude and with the Doctor Europaeus label) in Information and Communication Technology (Applied Electromagnetics curriculum) from both Sapienza University of Rome and Université de Rennes 1, Rennes, France, under a cotutelle agreement. In 2014, 2017, 2018, he was a Visiting Researcher and in 2023 a Visiting Scientist with the NATO-STO Center for Maritime Research and Experimentation, La Spezia, Italy. In 2016, he was a Visiting Researcher with the University of Houston, Houston, TX, USA. From July 2017 to June 2020, he was a Research Fellow at Sapienza University of Rome, and in July 2020, he joined the Institute for Microelectronics and Microsystems (IMM), Rome of the National Research Council of Italy as a Researcher, where he is currently a Senior Researcher since 2023. His current research interests include propagation of leaky, surface, and plasmonic waves, analysis and design of leaky-wave antennas, generation of electromagnetic localized waves, THz technology and spectroscopy, graphene electromagnetics, and metasurfaces. Dr. Fuscaldo was awarded several prizes, among which are the Young Engineer Prize for the Best Paper presented at the 46th European Microwave Conference in 2016, London, UK and and the Best Paper in Electromagnetics and Antenna Theory at the 12th European Conference on Antennas and Propagation in 2018.



David R. Jackson was born in St. Louis, MO on March 28, 1957. He obtained the B.S.E.E. and M.S.E.E. degrees from the University of Missouri, Columbia, in 1979 and 1981, respectively, and the Ph.D. degree in electrical engineering from the University of California, Los Angeles, in 1985. From 1985 to 1991, he was an Assistant Professor in the Department of Electrical and Computer Engineering at the University of Houston, Houston, TX. From 1991 to 1998, he was an Associate Professor in the same department, and since 1998 he has been a Professor in this department. He has been a Fellow of the IEEE since 1999. His present research interests include microstrip antennas and circuits, leaky-wave antennas, wave propagation effects including surface waves and leaky waves, leakage and radiation effects in microwave integrated circuits, periodic structures, and electromagnetic compatibility and interference. He serves on the IEEE Antennas and Propagation Society (AP-S) Committee on Promoting Equality (COPE) and on the MTT-1 (Microwave Field Theory) Technical Committee of the Microwave Theory and Technology Society. He is also serving as the Vice Chair of the IEEE AP-S Constitution and Bylaws Committee. Previously, he has served as the chair of USNC-URSI (The United States National Committee for the International Union of Radio Science). He has been the chair of the Distinguished Lecturer Committee of the IEEE AP-S, the chair of the Transnational Committee of the IEEE AP-S, the chair of the Chapter Activities Committee of the AP-S, a Distinguished Lecturer for the AP-S, a member of the AdCom for the AP-S, and an Associate Editor for the IEEE Transactions on Antennas and Propagation. He has also served as the chair of Commission B of USNC-URSI and as the Secretary of this Commission. He also previously served as an Associate Editor for the Journal Radio Science and the International Journal of RF and Microwave Computer-Aided Engineering.



Alessandro Galli received the Laurea degree in Electronic Engineering and the Ph.D. degree in Applied Electromagnetics from Sapienza University of Rome, Italy. Since 1990, he has been with the Department of Information Engineering, Electronics and Telecommunications of the same university. In 2000, he became an Assistant Professor and in 2002 an Associate Professor in the sector of Electromagnetic Fields; in 2012, he passed the National Scientific Qualification and then definitively achieved the role of Full Professor in the same sector and university. He authored about 300 papers in indexed journals, books, and conference proceedings. His research interests include theoretical and applied electromagnetics, mainly focused on modeling, numerical analysis, and design of antennas and passive devices from microwaves to terahertz. His research activities also concern the areas of geoelectromagnetics, bioelectromagnetics, and plasma heating. Dr. Galli was the Italian representative of the Board of Directors of the European Microwave Association (EuMA) from 2010 to 2015. He was the recipient of various grants and prizes for his research activity; in 2017, he was elected as the "Best Teacher" of the European School of Antennas (ESoA).

https://doi.org/10.1017/S1759078724001338 Published online by Cambridge University Press